

# A supersimple analysis of $e^-e^+ \rightarrow t\bar{t}$ at high energy.

G.J. Gounaris<sup>a</sup> and F.M. Renard<sup>b</sup>

<sup>a</sup>Department of Theoretical Physics, Aristotle University of Thessaloniki,  
Gr-54124, Thessaloniki, Greece.

<sup>b</sup>Laboratoire Univers et Particules de Montpellier, UMR 5299  
Université Montpellier II, Place Eugène Bataillon CC072  
F-34095 Montpellier Cedex 5.

## Abstract

According to supersimplicity in MSSM, a renormalization scheme (SRS) may be defined for any high energy 2-to-2 process, to the 1loop EW order; where the helicity conserving (HC) amplitudes, are expressed as a linear combination of just three universal logarithm-involving forms. All other helicity amplitudes vanish asymptotically. Including to these SRS amplitudes the corresponding counter terms, the "supersimple" expressions for the high energy HC amplitudes, renormalized on-shell, are obtained.

Previously, this property was noted for a large number of processes that do not involve Yukawa interactions or renormalization group corrections. Here we extend it to  $e^-e^+ \rightarrow t\bar{t}$ , which does involve large Yukawa and renormalization group contributions. We show that the resulting "supersimple" expressions may provide an accurate description, even at energies comparable to the SUSY scale. Such descriptions clearly identify the origin of the important SUSY effects, and they may be used for quickly constraining physics contributions, beyond MSSM.

PACS numbers: 12.15.-y, 12.15.-Lk, 12.60.Jv, 14.80.Ly

# 1 Introduction

In a recent paper [1], we have shown that at the 1loop EW order of several high energy 2-to-2 processes in MSSM, a remarkably simple structure arises for the helicity conserving<sup>1</sup> (HC) amplitudes; which are the only surviving amplitudes in this limit [2, 3]. This structure, which has been called "supersimplicity", involves just three forms: two Sudakov-like forms, containing a log or a log-squared function of the ratio of a Mandelstam variable with respect to masses, together with an additional energy independent term; and a squared-log of the ratio of two Mandelstam variables, to which  $\pi^2$  is added.

In [1], a supersimplicity renormalization scheme (SRS) was defined, where the high energy HC amplitudes exactly have the above "supersimplicity" structure, without any additional term. Adding to this "supersimplicity" amplitudes, some "residual" constant contributions, which are viewed as counter terms (c.t.); the "supersimple" expressions for the high energy HC amplitudes in the on-shell renormalization scheme [4] are obtained.

Such "supersimple" results arise in MSSM after many cancelations, among much more complicated contributions, involving standard and supersymmetric particle exchanges. While deriving them, it is fascinating to observe how the SUSY couplings conspire to achieve the supersimple structure for the high energy on-shell HC amplitudes, and at the same time to force the helicity violating (HV) amplitudes to vanish [1].

In SM, where such conspiracies do not appear, additional linear logarithms of ratios of Mandelstam variables arising from boxes appear [1], which cannot be thought as a combination of Sudakov-like forms [5, 6, 7, 8]. Furthermore, additional residual constants are needed to describe the high energy (on-shell renormalized) HC amplitudes; while nothing is generally known, for the HV amplitudes.

The supersimplicity structure was shown in [1] for a large number of MSSM processes, which did not involve any Yukawa terms or renormalization group corrections, to the electroweak (EW) couplings. For  $ug \rightarrow dW^+$  in particular, the supersimple high energy expressions for the HC amplitudes were considered in some detail. Such expressions were found to provide an accurate description, even at energies comparable to the SUSY scale [1].

In the present work we extend the analysis of [1], to a process involving renormalization group contributions and large Yukawa terms. Assuming that sometime in the future a high energy  $e^-e^+$  collider (LC) will be built, we consider the 1loop EW corrections to the process

$$e^-(l, \lambda) + e^+(l', \lambda') \rightarrow t(p, \mu) + \bar{t}(p', \mu') \quad , \quad (1)$$

where  $(l, l', p, p')$  denote the momenta, and  $(\lambda, \lambda', \mu, \mu')$  the helicities of the incoming and outgoing particles. The corresponding helicity amplitudes, denoted as

$$F(e^-e^+ \rightarrow t\bar{t})_{\lambda\lambda'\mu\mu'} \quad , \quad (2)$$

---

<sup>1</sup>The definitions of the HC and HV amplitudes appear in [1] and are repeated below.

are separated into two classes: the helicity conserving (HC) amplitudes satisfying

$$\lambda + \lambda' = \mu + \mu' \quad ; \quad (3)$$

and the helicity violating ones (HV), where (3) is not respected. Provided we ignore<sup>2</sup> CP-violating couplings in MSSM, the amplitudes (2) satisfy [9, 10, 11]

$$F(e^-e^+ \rightarrow t\bar{t})_{\lambda,\lambda',\mu,\mu'} = F(e^-e^+ \rightarrow t\bar{t})_{-\lambda',-\lambda,-\mu',-\mu} \quad . \quad (4)$$

Process (1), indeed involves large Yukawa interactions affecting the final  $t\bar{t}$  state; while the existence of gauge boson self-energy contributions, generates renormalization group (RG) logs and large  $\Delta\rho$ -type terms<sup>3</sup>. Our purpose is to investigate how supersimplicity is affected by such contributions.

Neglecting the electron mass, non-vanishing helicity amplitudes always satisfy  $\lambda + \lambda' = 0$ , which combined with (4), means that there exist only two independent HV amplitudes, for which we take  $F_{-+-}$ ,  $F_{+--}$ . As discussed in connection to Fig.2, these HV amplitudes are quickly depressed at high energies in MSSM, in agreement with the general expectations [2, 3].

On the contrary, the helicity conserving (HC) amplitudes, denoted as

$$F_{-++} \quad , \quad F_{+--} \quad , \quad F_{-+-} \quad , \quad F_{+--} \quad , \quad (5)$$

remain appreciable at high energies. Explicit high energy supersimple expressions for them are given in Appendix A. In constructing them, we separate the HC amplitudes into two parts, defined in Sect. 2. The first one, called "augmented Sudakov" part, contains contributions from the triangles, boxes and the electron and top-quark self-energy counter-terms (c.t.); while the second part, called "augmented renormalization group (RG)" part, is obtained from the  $\gamma\gamma$ ,  $\gamma Z$  and  $ZZ$  renormalized self-energy bubbles, exchanged in the  $s$ -channel.

These two parts are respectively denoted as  $F_{\lambda\lambda'\mu\mu'}^{\text{Sud}}$  and  $F_{\lambda\lambda'\mu\mu'}^{\text{s.e.}}$ . As discussed in Sect. 2, the independence of this separation from the gauge fixing procedure, is guaranteed by subtracting from  $F_{\lambda\lambda'\mu\mu'}^{\text{Sud}}$  the pinch part of the triangular graphs in Fig.1, and including it in  $F_{\lambda\lambda'\mu\mu'}^{\text{s.e.}}$  [12, 13].

In Sect. 3 and Appendix A, we discuss our predictions for the HV and HC amplitudes for process  $e^-e^+ \rightarrow t\bar{t}$ , in MSSM models. As examples of the way such expressions may be used in studying physically observable quantities, we consider the differential cross section  $d\sigma(e^-e^+ \rightarrow t\bar{t})/d\cos\theta$ , the forward-backward ( $A_{FB}$ ) and the left-right ( $A_{LR}^t$ ) asymmetries. It is then argued that the supersimple MSSM expressions for the HC amplitudes, may be useful for quickly distinguishing SUSY contributions from possible new physics contributions induced e.g. by a new  $Z'$  vector or axial boson, or by new anomalous  $Zt\bar{t}$  couplings.

Finally in the fourth section we give our conclusions and discuss the theoretical aspects and the implications of our results.

---

<sup>2</sup>As we have done also in [1].

<sup>3</sup>See Sect. 3.2

## 2 The augmented Sudakov and RG forms.

As explained in the Introduction, the "augmented Sudakov" part of the HC amplitudes, denoted as  $F_{\lambda\lambda'\mu\mu'}^{\text{Sud}}$ , contains the contributions from the triangles and boxes, as well as the contributions from the counter-terms (c.t.) related to the external  $(e^-, e^+, t, \bar{t})$  particles. To ensure gauge invariance though, we have subtracted from them, the pinch part of the  $W\nu_e W$  and  $WbW$  triangles, indicated in Fig.1 [12, 13]. This "pinch" term handling, only affects  $F_{-++}$ .

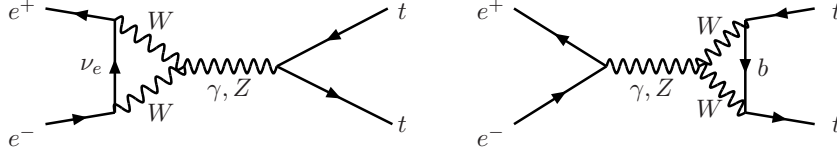


Figure 1: Diagrams contributing to the pinch term.

Apart from  $F_{\lambda\lambda'\mu\mu'}^{\text{Sud}}$ , there exists also the  $F_{\lambda\lambda'\mu\mu'}^{\text{s.e.}}$  part of the HC amplitudes, called "augmented RG" part. This contains the contributions from the  $\gamma\gamma$ ,  $\gamma Z$  and  $ZZ$  renormalized self-energy bubbles in the  $s$ -channel, and includes also the pinch term mentioned above.

An easy way to calculate both these amplitude-parts at high energy, is by studying the SUSY-transformed process  $\tilde{e}^-\tilde{e}^+ \rightarrow \tilde{t}\tilde{t}$  [1]. But in order to unambiguously obtain all constant terms, a direct 1loop computation of the  $e^-e^+ \rightarrow t\bar{t}$  amplitudes is also made, following [14] and using the asymptotic expansion [15] of the Passarino-Veltman (PV) functions [16].

Denoting by  $x, y$ , any two of the Mandelstam variables  $(s, t, u)$  in  $e^-e^+ \rightarrow t\bar{t}$ , while  $V = \gamma, Z, W$ , we find that a supersimplicity renormalization scheme (SRS) may be defined in MSSM. In this SRS scheme, the high energy 1loop HC amplitudes are given by a linear combination of the forms

$$\overline{\ln^2 x_V} \equiv \ln^2 x_V + 2L_{a_1 V c_1} + 2L_{a_2 V c_2} \quad , \quad x_V \equiv \left( \frac{-x - i\epsilon}{m_V^2} \right) \quad , \quad (6)$$

$$\overline{\ln x_{ij}} \equiv \ln x_{ij} + b_0^{ij}(m_a^2) - 2 \quad , \quad \ln x_{ij} \equiv \ln \frac{-x - i\epsilon}{m_i m_j} \quad , \quad (7)$$

$$\ln^2 r_{xy} + \pi^2 \quad , \quad r_{xy} \equiv \frac{-x - i\epsilon}{-y - i\epsilon} \quad , \quad (8)$$

with the coefficients of the Sudakov forms (6) and (7) being constants, satisfying the general constraints [5, 6, 7, 8]; while the coefficients of (8) may also contain ratios of Mandelstam variables, as well as constants. No additional overall terms can exist in the SRS HC amplitudes [1]. This structure is exactly the same as in [1]. Such SRS HC amplitudes are related to the on-shell renormalization scheme ones [4], through an additional residual

constant contribution [1]. The expressions for the on-shell HC amplitudes thus obtained, are the "supersimple" expressions mentioned above and given in Appendix A.

We next discuss the forms (6-8). As shown in [1], the augmented Sudakov squared-logs appearing in (6) are always associated to triangles or boxes involving gauge exchanges ( $V = \gamma, Z, W$ ). In particular the  $L_{a_i V c_i}$  terms appearing there, are defined by

$$L_{aVc} \equiv L(p_a, m_V, m_c) = \text{Li}_2 \left( \frac{2p_a^2 + i\epsilon}{m_V^2 - m_c^2 + p_a^2 + i\epsilon + \sqrt{\lambda(p_a^2 + i\epsilon, m_V^2, m_c^2)}} \right) + \text{Li}_2 \left( \frac{2p_a^2 + i\epsilon}{m_V^2 - m_c^2 + p_a^2 + i\epsilon - \sqrt{\lambda(p_a^2 + i\epsilon, m_V^2, m_c^2)}} \right) , \quad (9)$$

where  $\text{Li}_2$  is a Spence function and

$$\lambda(a, b, c) = a^2 + b^2 + c^2 - 2ab - 2ac - 2bc . \quad (10)$$

Note that in  $L_{a_i V c_i}$  in (6), the gauge boson always appears as a middle index; while  $a_i$  describes an external particle of  $e^- e^+ \rightarrow t \bar{t}$ ; and  $c_i$  denotes an internal exchange in the diagram generating the specific high energy term [5, 6, 7, 8].

We next turn to augmented Sudakov linear logs in (7). The constant contribution  $b_0^{ij}(m_a^2)$  in them, is determined by the finite part of the  $B_0^{ij}(m_a^2)$  PV function [16, 1]

$$b_0^{ij}(m_a^2) \equiv b_0(m_a^2; m_i, m_j) = 2 + \frac{1}{m_a^2} \left[ (m_j^2 - m_i^2) \ln \frac{m_i}{m_j} + \sqrt{\lambda(m_a^2 + i\epsilon, m_i^2, m_j^2)} \text{ArcCosh} \left( \frac{m_i^2 + m_j^2 - m_a^2 - i\epsilon}{2m_i m_j} \right) \right] , \quad (11)$$

where  $(i, j)$  describe two internal exchanges, while  $m_a$  denotes the mass of either an external particle ( $e^\mp, t, \bar{t}$ ), or a neutral gauge boson ( $V = \gamma, Z$ ), that can couple to the  $ij$ -pair.

The first case, where  $b_0^{ij}(m_a^2)$  is associated to an external line, arises from the cancellation between the divergences

$$\Delta - \ln + b_0^{ij}(m_a^2) , \quad (12)$$

induced by triangular diagrams, and those induced by the  $e, t$  counter terms (c.t.), finally leading to expressions like  $\ln + b_0^{ij}(m_a^2) - c$ , where  $c$  is a pure number. But then a remarkable property appears in SUSY, where only the HC amplitudes need to be considered [2, 3]. For each group of related diagrams, the value of  $c$  induced by the SM-exchanges differs from the one induced by the the pure SUSY ones. It is only when all related diagrams are combined, that the sum of the SM and SUSY contributions produces the value  $c = 2$  appearing in (7) [1].

A few typical examples are:

- For triangles involving a single gauge exchange related to the initial  $e^\mp$  lines and their (c.t.), the gauge exchanges contribute  $3\ln + 3b_0^{Vf}(m_e^2) - 7$ , with ( $f = e, \nu_e$ ) and ( $V = W, Z, \gamma$ ). The corresponding SUSY gaugino-slepton exchanges give  $-\ln - b_0^{\tilde{V}\tilde{f}}(m_e^2) + 3$ . Adding the two, the MSSM total result becomes a combination of forms like  $[\ln + b_0^{ij}(m_e^2) - 2]$ .
- For Yukawa triangles connected to the final  $(t, \bar{t})$  lines and their (c.t.), the SM Higgs exchanges produce terms like  $-\ln - b_0(m_t^2) + 3$ , while the SUSY additional Higgs and higgsino exchanges contribute  $-\ln - b_0(m_t^2) + 1$ , so that the MSSM total is again a combination of forms like  $[\ln + b_0(m_t^2) - 2]$ .

The second case where in (7) we have  $m_a = m_\gamma, m_Z$ , was never seen in the processes studied in [1]. It is first observed here for  $e^-e^+ \rightarrow t\bar{t}$ . Regularizing the infrared singularities by choosing  $m_\gamma = m_Z$  [1], we thus encounter additional augmented Sudakov linear logs like

$$\begin{aligned}
\overline{\ln s_{WW}} &= \ln s_{WW} + b_0^{WW}(m_z^2) - 2 \quad , \\
\overline{\ln s_{H^+H^-}} &= \ln s_{H^+H^-} + b_0^{H^+H^-}(m_z^2) - 2 \quad , \\
\overline{\ln s_{h^0Z}} &= \ln s_{h^0Z} + b_0^{h^0Z}(m_z^2) - 2 \quad , \\
\overline{\ln s_{H^0Z}} &= \ln s_{H^0Z} + b_0^{H^0Z}(m_z^2) - 2 \quad , \\
\overline{\ln s_{h^0A^0}} &= \ln s_{h^0A^0} + b_0^{h^0A^0}(m_z^2) - 2 \quad , \\
\overline{\ln s_{H^0A^0}} &= \ln s_{H^0A^0} + b_0^{H^0A^0}(m_z^2) - 2 \quad , \\
\overline{\ln s_{ff}} &= \ln s_{ff} + b_0^{ff}(m_z^2) - 2 \quad , \\
\overline{\ln s_{\tilde{f}_i\tilde{f}_j}} &= \ln s_{\tilde{f}_i\tilde{f}_j} + b_0^{\tilde{f}_i\tilde{f}_j}(m_z^2) - 2 \quad , \\
\overline{\ln s_{\tilde{\chi}_i\tilde{\chi}_j}} &= \ln s_{\tilde{\chi}_i\tilde{\chi}_j} + b_0^{\tilde{\chi}_i\tilde{\chi}_j}(m_z^2) - 2 \quad , 
\end{aligned} \tag{13}$$

where the indices  $(i, j)$  in  $\ln s_{ij}$ , describe particles with non-vanishing  $\gamma_{ij}$  or  $Z_{ij}$  couplings. Such terms are generated by counter terms in the  $\gamma, Z$  self energy insertions  $\Sigma_{\gamma\gamma}(s)$ ,  $\Sigma_{\gamma Z}(s)$  and  $\Sigma_{ZZ}(s)$ . More explicitly, the gauge self-energy insertions give contributions like  $-\Delta + \ln - 2$ , whose  $\Delta$ -divergence is canceled by quantities like  $\Delta + b_0^{ij}(m_Z^2) - \ln(m_i m_j / \mu^2)$ , induced by the gauge wave function renormalization constants [15]. This is similar to the case discussed around (12), where the divergences are canceled by the electron or top counter terms.

We also remark that the terms in (13) concern only the pinch and the augmented RG parts of the high energy HC amplitudes. The augmented Sudakov contributions to the high energy HC amplitudes, do not have this form.

As a result, the  $\overline{\ln s_{WW}}$  term in the  $F_{-+-+}^{\text{Sud}}$  expression (A.5), is directly related to the subtraction of the pinch contribution from the diagrams in Fig.1 [12, 13]. Its magnitude is given by

$$\frac{\alpha^2}{s_W^4} \overline{\ln s_{WW}} \quad . \tag{14}$$

It is this term that has been subtracted from the definitions of  $F_{-+-+}^{\text{Sud}}$ , and inserted in  $F_{-+-+}^{\text{s.e.}}$  given in (A.10). None of the other high energy HC amplitudes  $F_{\lambda\lambda'\mu\mu'}^{\text{Sud}}$ , is affected by terms in (13).

In contrast to this, all forms (13) contribute to the augmented RG parts of the asymptotic HC amplitudes  $F_{\lambda\lambda'\mu\mu'}^{\text{s.e.}}$ .

Finally, in addition to the augmented squared and linear logs scaled by masses, a third form given by (8), also appears in the high energy HC amplitudes [1]. Typical expressions of this kind, for both  $\tilde{e}^-\tilde{e}^+ \rightarrow \tilde{t}\tilde{t}$  and  $e^-e^+ \rightarrow t\bar{t}$  processes, are  $(\ln^2 r_{us} + \pi^2)$  or  $(\ln^2 r_{ts} + \pi^2)$ , always arising purely from boxes.

### 3 The HC amplitudes for $e^-e^+ \rightarrow t\bar{t}$ .

In this Section we discuss the exact 1loop EW results for the  $F_{\lambda\lambda'\mu\mu'}^{\text{Sud}}$  and  $F_{\lambda\lambda'\mu\mu'}^{\text{s.e.}}$  parts of the HC amplitudes in MSSM, and compare them to the corresponding high energy supersimple expressions given in Appendices A.1 and A.2 respectively. The results in (A.5-A.8) and (A.10-A.13) clearly indicate that the Yukawa interactions and the RG contributions, do respect the supersimplicity structure.

As we show below, these supersimple expressions reproduce the main features of the exact 1loop amplitudes, even for energies close to the SUSY scale.

For assessing this explicitly, we first show the quick vanishing, as the energy increases, of the HV amplitudes. Then, we turn to the augmented Sudalov part of the HC amplitudes and compare the exact 1loop results for  $F_{\lambda\lambda'\mu\mu'}^{\text{Sud}}$ , with the corresponding supersimple high energy expressions in Appendix A.1. And once this is done, we turn to the complete amplitudes

$$F_{\lambda\lambda'\mu\mu'} = F_{\lambda\lambda'\mu\mu'}^{\text{Sud}} + F_{\lambda\lambda'\mu\mu'}^{\text{s.e.}} \quad , \quad (15)$$

and compare them to their supersimple approximation obtained by summing the corresponding expressions in Appendices A.1 and A.2.

For the numerical illustrations, we use two MSSM benchmarks, consistent with the present LHC results. The first, called MSSMhigh, is given by the cMSSM high scale parameters [17]

$$m_0 = 1080 \quad , \quad m_{1/2} = 1800 \quad , \quad A_0 = 860 \quad , \quad \tan\beta = 48 \quad , \quad \mu > 0 \quad , \quad (16)$$

where all dimensional quantities are in GeV. For this model, the SuSpect code gives  $m_{h^0} \simeq 122$  GeV, while the lightest neutralino is put at about 800 GeV, and all other SUSY particles acquire masses between 1000 and almost 4000 GeV [18]. As a result, the SUSY contribution to  $(g_\mu - 2)/2$  is tiny, in this benchmark.

The second benchmark, called MSSMlow, is characterized by the EW scale parameters [19, 20]

$$\begin{aligned} M_1 &= 100 \quad , \quad M_2 = 200 \quad , \quad M_3 = 800 \quad , \\ m_{\tilde{l}} &= 400 \quad , \quad m_{\tilde{q}} = 1100 \quad , \quad A_\tau = -800 \quad , \quad A_b = A_t = -2200 \quad , \\ \mu &= 200 \quad , \quad m_{A^0} = 320 \quad , \quad \tan \beta = 20 \quad , \end{aligned} \quad (17)$$

where  $m_{\tilde{l}}, m_{\tilde{q}}$  describe the common EW scale SUSY breaking slepton and squark masses, for all three generations; (again all masses in GeV). The charginos, neutralinos and sleptons in MSSMlow are much lighter than in the previous benchmark. Consequently, this benchmark can accommodate a large SUSY contribution to  $(g_\mu - 2)/2$ , consistent with the experimental data [21, 22]. Moreover, SuSpect [18] gives for it  $m_{h^0} \simeq 125$  GeV, the lightest neutralino is put at 90 GeV, and the  $m_{A^0}$  and  $m_{H^0}$  masses are in the 320 GeV region [20].

Using these two MSSM benchmarks<sup>4</sup>, we present in Fig.2, the two independent HV amplitudes  $F_{-+--}$ ,  $F_{+---}$ , as functions of energy, at a fixed c.m. angle  $\theta = 60^\circ$ . As seen there, the 1loop EW order results for both HV amplitudes, as well as their Born approximation, are almost identical and quickly suppressed at high energies, in agreement with the general helicity-conservation (HCns) theorem [2, 3].

We conclude therefore that for a quick study of physical observables, it may be sufficient to use the Born approximation for the HV amplitudes.

### 3.1 The $F_{\lambda\lambda'\mu\mu'}^{\text{Sud}}$ part of the HC amplitudes.

We first investigate whether the exact 1loop results for  $F_{\lambda\lambda'\mu\mu'}^{\text{Sud}}$  agree with the corresponding supersimple expressions, at asymptotic energies. In other words, whether there are any residual contributions that they should still be added to the expressions in Appendix A.1. Such residual contributions are essentially determined by the differences between the  $e$  or  $t$  wave function renormalization constants, in the on-shell [4] and SRS renormalization schemes [1],

$$\delta Z_f^{L,R, \text{res}} = Z_f^{L,R, \text{OS}} - Z_f^{L,R, \text{SRS}} \quad , \quad (18)$$

where  $f = e, t$ . For this we find for MSSMlow (17)

$$\begin{aligned} \delta Z_e^{L, \text{res}} &= -0.00091 \quad , \quad \delta Z_e^{R, \text{res}} = -0.00243 \quad , \\ \delta Z_t^{L, \text{res}} &= 0.00202 \quad , \quad \delta Z_t^{R, \text{res}} = 0.00196 \quad , \end{aligned} \quad (19)$$

while for MSSMhigh (16)

$$\begin{aligned} \delta Z_e^{L, \text{res}} &= -0.00039 \quad , \quad \delta Z_e^{R, \text{res}} = -0.00124 \quad , \\ \delta Z_t^{L, \text{res}} &= 0.00330 \quad , \quad \delta Z_t^{R, \text{res}} = 0.00051 \quad . \end{aligned} \quad (20)$$

---

<sup>4</sup>A very short list of other possible benchmarks may be found in [23].



Thus  $|\delta Z_f^{L,R, \text{res}}| \ll 1$ , which means that no further residual terms are needed in (A.5-A.8).

In Fig.3 we then present the energy dependence of the augmented Sudakov part of the HC amplitudes  $F_{\lambda\lambda'\mu\mu'}^{\text{Sud}}$ . The c.m. scattering angle is fixed at  $\theta = 60^\circ$ . Full lines describe the exact 1loop EW order results; while broken lines, indicated by "sim", denote the supersimple high energy amplitudes in Appendix A.1.

As seen in this figure, the differences between the exact and supersimple results, are almost invisible for all HC augmented Sudakov amplitudes, at all energies, for the MSSM models (17, 16). In fact, at energies in the range  $0.4 \lesssim \sqrt{s} \lesssim 1$  TeV, some visible differences only appear for  $F_{-++-}^{\text{Sud}}$ ; but they become invisible for  $\sqrt{s} \gtrsim 1$  TeV.

Therefore, the the supersimple expressions for the augmented Sudakov amplitudes in Appendix A.1, approach the corresponding exact 1loop results, very quickly, for the above MSSM benchmarks.

### 3.2 The $F_{\lambda\lambda'\mu\mu'}^{\text{s.e.}}$ part of the HC amplitudes.

As already said in Sect.2, the augmented RG part for the HC amplitudes  $F_{\lambda\lambda'\mu\mu'}^{\text{s.e.}}$ , describes the 1loop finite contribution arising from the renormalized  $\gamma\gamma$ ,  $\gamma Z$  and  $ZZ$  self-energy functions, together with the pinch contribution of the graphs in Fig.1. The high energy supersimple expressions for these  $e^-e^+ \rightarrow t\bar{t}$  amplitudes appear in Appendix A.2.

Using the definitions in Appendix A.2 and (A.4), we first check that the logarithms of this part coincide with those in the renormalization group result

$$F^{\text{RG log}} = -\frac{1}{4\pi^2} \ln\left(\frac{s}{m_Z^2}\right) \left[ \beta_2 g_2^4 \left( \frac{dF^{\text{Born}}}{dg_2^2} \right) + \beta_1 g_1^4 \left( \frac{dF^{\text{Born}}}{dg_1^2} \right) \right] , \quad (21)$$

where  $g_1 = e/c_W$ ,  $g_2 = e/s_W$  and

$$\beta_1 = \frac{-11}{4} \quad , \quad \beta_2 = \frac{-1}{4} \quad , \quad (22)$$

leading to

$$\begin{aligned} F_{-++-}^{\text{RG log}} &= \alpha^2 \left( \frac{2u}{s} \right) \left[ \frac{-3 + 6s_W^2 - 14s_W^4}{12s_W^4 c_W^4} \right] \ln\left(\frac{s}{m_Z^2}\right) , \\ F_{+--+}^{\text{RG log}} &= \alpha^2 \left( \frac{2u}{s} \right) \left[ \frac{-22}{3c_W^4} \right] \ln\left(\frac{s}{m_Z^2}\right) , \\ F_{-+-+}^{\text{RG log}} &= \alpha^2 \left( \frac{-2t}{s} \right) \left[ \frac{11}{3c_W^4} \right] \ln\left(\frac{s}{m_Z^2}\right) , \\ F_{+---}^{\text{RG log}} &= \alpha^2 \left( \frac{-2t}{s} \right) \left[ \frac{11}{6c_W^4} \right] \ln\left(\frac{s}{m_Z^2}\right) , \end{aligned} \quad (23)$$

which indeed agree with the logarithmic terms in (A.10-A.13).

We next discuss the energy independent residual terms, that are needed in the supersimple expressions (A.17,A.18,A.19); in order to describe the exact 1loop values for  $\hat{\Sigma}_{\gamma\gamma}$ ,  $\hat{\Sigma}_{\gamma Z}$ ,  $\hat{\Sigma}_{ZZ}$ , at asymptotic energies.

For  $\hat{\Sigma}_{\gamma\gamma}(s)$ , no such term is needed in (A.17).

But for  $\hat{\Sigma}_{\gamma Z}(s)$  and  $\hat{\Sigma}_{ZZ}(s)$ , a quantity like

$$\overline{\Delta\rho} \simeq 0.017 \quad , \quad (24)$$

is needed in (A.18,A.19), for the MSSM benchmarks (17, 16). This value is close to the well-known neutral-to-charged current ratio parameter

$$\Delta\rho = \frac{\Sigma^{ZZ}(0)}{m_Z^2} - \frac{\Sigma^{WW}(0)}{m_W^2} \sim 0.01 \quad , \quad (25)$$

mainly determined by the  $(b, t)$  contributions. Such a similarity is not be accidental, since the structure of (A.14, A.15) suggests that gauge self-energy differences like those in (25), play an important role in determining the value of  $\overline{\Delta\rho}$ , thereby motivating its name.

Taking into account the  $\overline{\Delta\rho}$ -contributions in (A.18,A.19), the differences between the exact 1loop contribution to the  $F_{\lambda\lambda'\mu\mu'}^{\text{s.e.}}$  part of the HC amplitudes, and the supersimple expressions (A.10-A.13), normalized to the corresponding Born contributions, are

- for MSSMlow (17)

$$\begin{aligned} \delta F_{-++-}^{\text{s.e.}}/F_{-++-}^{\text{Born}} &= 0.00054 \quad , & \delta F_{+--+}^{\text{s.e.}}/F_{+--+}^{\text{Born}} &= -0.00303 \quad , \\ \delta F_{-++-}^{\text{s.e.}}/F_{-++-}^{\text{Born}} &= 0.00266 \quad , & \delta F_{+--+}^{\text{s.e.}}/F_{+--+}^{\text{Born}} &= 0.01406 \quad , \end{aligned} \quad (26)$$

- while for MSSMhigh (16)

$$\begin{aligned} \delta F_{-++-}^{\text{s.e.}}/F_{-++-}^{\text{Born}} &= -0.00128 \quad , & \delta F_{+--+}^{\text{s.e.}}/F_{+--+}^{\text{Born}} &= -0.00413 \quad , \\ \delta F_{-++-}^{\text{s.e.}}/F_{-++-}^{\text{Born}} &= 0.00162 \quad , & \delta F_{+--+}^{\text{s.e.}}/F_{+--+}^{\text{Born}} &= 0.01313 \quad . \end{aligned} \quad (27)$$

The results (26, 27) guarantee that the supersimple expressions (A.10-A.13) accurately approximate the exact 1loop results for the  $F_{\lambda\lambda'\mu\mu'}^{\text{s.e.}}$  HC amplitudes at high energies. That is, no further residual terms are needed in (A.10-A.13), at least for the two above benchmarks.

### 3.3 The complete HC amplitudes

We next turn to the complete HC amplitude given in (15).

In Fig.4, we present the energy dependence at  $\theta = 60^\circ$ , of the complete HC amplitudes  $F_{-++-}$ ,  $F_{+--+}$  (upper panels), and  $F_{-++-}$ ,  $F_{+--+}$  (lower panels), in the benchmarks

MSSMhigh (16) and MSSMlow (17). For comparison, the exact 1loop SM results are also given. Left panels show the 1loop effects on Born, in SM and MSSM; note that above 1 TeV, the 1loop effects strongly depend on the HC amplitude considered, acquiring their largest values for  $F_{-++-}$ . Right panels give a feeling of how accurately the supersimple expressions approximate the exact 1loop results in the energy range from the  $t\bar{t}$ -threshold to 7 TeV, for the aforementioned MSSM benchmarks. For  $F_{+--+}$ ,  $F_{+--+}$  this accuracy is rather good for both benchmarks. For MSSMlow, good accuracy also exists for both  $F_{-++-}$ ,  $F_{-++-}$ . For MSSMhigh though, discrepancies at the 1% level persist for  $F_{-++-}$ , even for  $\sqrt{s} \gtrsim 7$  TeV; while for  $F_{-++-}$ , the accuracy improves at  $\sqrt{s} \gtrsim 4.5$  TeV. These features are due to the high value (around 3 TeV) of the SUSY scale in MSSMhigh, which delays the vanishing of the mass-suppressed contributions.

In Fig.5, we give illustrations for the energy dependence of the "dimensionless cross section" defined as

$$\sum_{\lambda\lambda'\mu\mu'} |F_{\lambda\lambda'\mu\mu'}(e^-e^+ \rightarrow t\bar{t})|^2 . \quad (28)$$

Full lines give the exact 1loop EW order results, while the broken lines give the "sim" predictions. By "sim" in the case of (28) we mean that, the the supersimple results of Appendix A are used for the HC amplitudes, while for the HV ones the Born expressions are used.

As seen in the left panel of Fig.5, the exact and "sim" contributions for MSSMlow, are very similar. For MSSMhigh though, the right panel of Fig.5 indicates a change of sign for the (exact-"sim") difference at around 3 TeV, again related to the value of the SUSY scale in this benchmark; compare the right panels Fig.4.

Similar patterns for MSSMlow and MSSMhigh also appear in Fig.6 and Fig.7, where the angular dependence of the "dimensionless cross section" (28) are shown. For MSSMhigh in particular, the (exact-"sim") difference is at the 2% level for 1 TeV c.m. energy, while it reaches the 1% level at about 10 TeV.

In order to show how these supersimple expressions can be used for quickly disentangling the supersymmetric effects, from other possible non standard contributions, we now consider two such examples: an anomalous  $Zt\bar{t}$  coupling described by the effective interaction in (B.1); and an additional  $Z'$  with purely vector or axial couplings to electrons and top quarks (B.3). Such a possibility of anomalous top properties is open, after the Tevatron recent results [24, 25].

In Fig.7, we give the results for the case of an anomalous  $Zt\bar{t}$  coupling (B.1) with  $d^Z = \pm 0.15$ , causing the  $\sin\theta$ -proportional contribution to the HV amplitudes given in (B.2). As seen there, such a  $d^Z$  induces discrepancies, which are much larger and have a different structure from those of the (exact-"sim") differences caused by MSSMlow or MSSMhigh, alone. Thus, the supersimple expressions may be adequate for excluding such anomalous couplings.

Table 1: The  $A_{FB}$  and  $A_{LR}^t$  asymmetries for  $e^-e^+ \rightarrow t\bar{t}$ , in two MSSM benchmarks, at the exact 1loop EW order and the "sim" approximation. The results for adding to the exact 1loop predictions, a new physics contribution, are also shown.

$A_{FB}$						
	1loop	SIM	$d^z = 0.15$	$d^z = -0.15$	$Z'(V)$	$Z'(A)$
MSSM <sub>high</sub> [17]	0.855	0.859	0.776	0.725	0.813	0.916
MSSM <sub>low</sub> [19, 20]	0.868	0.859	0.790	0.743	0.828	0.921
$A_{LR}^t$						
	1loop	SIM	$d^z = 0.15$	$d^z = -0.15$	$Z'(V)$	$Z'(A)$
MSSM <sub>high</sub> [17]	0.271	0.293	0.237	0.219	0.222	0.279
MSSM <sub>low</sub> [19, 20]	0.264	0.287	0.232	0.216	0.218	0.266

Such a  $\sin\theta$ -proportional contribution to the HV amplitudes, as in (B.1,B.2), when combined with the MSSM contributions, may also change the forward-backward asymmetry  $A_{FB}$ , to which we now turn.

In addition to  $A_{FB}$ , we also consider the  $A_{LR}^t$  Left-Right asymmetry defined as

$$A_{LR}^t \equiv \frac{\sigma(e^-e^+ \rightarrow t_L\bar{t}) - \sigma(e^-e^+ \rightarrow t_R\bar{t})}{\sigma(e^-e^+ \rightarrow t_L\bar{t}) + \sigma(e^-e^+ \rightarrow t_R\bar{t})} , \quad (29)$$

where  $\sigma(e^-e^+ \rightarrow t_L\bar{t})$  and  $\sigma(e^-e^+ \rightarrow t_R\bar{t})$  describe the cross sections for the production of a  $t$ -quark with helicities  $\mu = -1/2$  and  $\mu = +1/2$ , respectively. All other polarizations in (29) are summed over.

The results for  $A_{FB}$  and  $A_{LR}^t$  are presented in Table 1. In detail: the second column gives the exact EW 1loop results for MSSM<sub>high</sub> and MSSM<sub>low</sub>; the third column gives the corresponding "sim" results, defined as in the Figs.6,7; the fourth and fifth columns give the effects of adding to the exact 1loop results, the anomalous HV amplitudes (B.2), with  $d^Z = \pm 0.15$ ; the sixth column gives the corresponding effect in case the only additional physics, beyond MSSM, consists of a  $Z'$  at 3TeV, coupled like in (B.3), with identical vector couplings to both  $e^-e^+$  and  $t\bar{t}$ ; while finally the seventh column gives the corresponding effect for an axial  $Z'$ .

Table 1 reaffirms the implications from Figs.5,6,7. The "sim" results, approximate the exact 1loop ones, for MSSM<sub>low</sub> or MSSM<sub>high</sub>, sufficiently well; so that a  $d^Z = \pm 0.15$  can be distinctly visible, even when the SUSY implications are described just by "sim".

Table 1 suggests that this is also true for discovering a 3 TeV  $Z'$  vector or axial contribution, of the kind appearing in (B.3).

The above two examples were chosen with arbitrary values of their parameters, just in order to illustrate the possibility to use the supersimple expressions, for detecting types of physics beyond MSSM.

## 4 Conclusions

In this paper, we have extended the supersimplicity concept to the MSSM process  $e^-e^+ \rightarrow t\bar{t}$ , where Yukawa interactions and renormalization group (RG) contributions play important roles. Such features do not exist in the originally considered processes in [1].

More explicitly, the "augmented Sudakov" structure found in [1], is also observed for the Yukawa part of the electroweak corrections. And the "augmented RG" structure induced by the photon and  $Z$  exchanges in the  $s$ -channel, together with the related pinch contributions, are also found to respect this supersimplicity structure, with specific  $\Delta\rho$  type residual contributions.

This supersimplicity realization is due to spectacular SUSY properties, arising from cancelations of virtual standard and spartner contributions, allowing to write simple expressions for the helicity conserving amplitudes at high energies. We have thus obtained very simple expressions for the high energy on-shell HC amplitudes, which we have termed "supersimple". At such high energies, the helicity violating amplitudes are found to be very small.

A numerical comparison of the "supersimple" expressions, with the exact 1loop results, shows that their accuracy is very good, even at energies comparable to the SUSY scale; at least for the two benchmarks MSSMhigh and MSSMlow, we have used in the illustrations. Both, the energy dependence and the angular distribution of the cross section presented respectively in Fig.5 and Figs.6,7, are very well reproduced. Only close to threshold, one may observe some (small) departures. This should remain true for any MSSM benchmark, provided the energy is sufficiently above the SUSY scale.

Comparing Fig.2 and 4 we can also see that for both MSSMhigh and MSSMlow at 1 TeV and  $\theta = 60^\circ$ , the HC amplitudes are already dominating the HV ones; so that the HV contribution to the cross sections is at the 3% level. Varying the angle, changes relative individual contributions from various HC and HV amplitudes; but globally the ratio of their contributions to the cross section remains at this level. Above 1 TeV of course, the HV contribution to the cross section falls quickly down.

These results have interesting theoretical and predictive implications.

Theoretically they emphasize the elegance of Supersymmetry, where the joint action of standard and of spartner states, produces remarkable structures for the amplitudes at high energy. More explicitly SUSY forces all helicity violating 2-to-2 amplitudes to vanish exactly at high energy [2, 3]; while it assigns to the HC amplitudes at the 1loop EW order, very simple and accurate expressions [1].

For a SUSY scale in the range of the above two benchmarks, the predictive power of the supersimple description reaches the accuracy of the percent level, at reasonable energies. It can therefore be used to calculate the values of physical observables, keeping the identification of the important physical input clear. In other words, without relying on enormous codes, where the main physical reason and the many minor effects, are thoroughly interwoven. For example, we have shown that the supersimplicity expressions

may be useful for immediately distinguished the MSSM effects, from possible top-related new physics, beyond it.

## A Appendix: High energy HC amplitudes

Defining the momenta and helicities for the  $e^-e^+ \rightarrow t\bar{t}$  process as in (1), and the helicity amplitudes as in (2), the Born contributions are given by

$$F_{\lambda\lambda'\mu\mu'}^{\text{Born}} = \sum_{V=\gamma,Z} \frac{1}{s - m_V^2} \bar{u}_t(p, \mu) \gamma^\mu (g_{Vt}^L P_L + g_{Vt}^R P_R) v_t(p', \mu') \cdot \bar{v}_e(l', \lambda') \gamma_\mu (g_{Ve}^L P_L + g_{Ve}^R P_R) u_e(l, \lambda) , \quad (\text{A.1})$$

where  $(l, l', p, p')$  denote the momenta and  $(\lambda, \lambda', \mu, \mu')$  the helicities, of the incoming and outgoing particles, using the standard conventions [9]. Neglecting all masses at high energies, the Mandelstam variables are

$$\begin{aligned} s &= (l + l')^2 = (p + p')^2 , \\ t &= (l - p)^2 = -\frac{s}{2}(1 - \cos \theta) , \\ u &= (l - p')^2 = -\frac{s}{2}(1 + \cos \theta) , \end{aligned} \quad (\text{A.2})$$

where  $\theta$  is the c.m. scattering angle. Finally

$$\begin{aligned} g_{\gamma e}^L &= g_{\gamma e}^R = -e , \quad g_{\gamma t}^L = g_{\gamma t}^R = \frac{2e}{3} , \\ g_{Ze}^L &= \frac{e(-1 + 2s_W^2)}{2s_W c_W} , \quad g_{Ze}^R = \frac{es_W}{c_W} , \\ g_{Zt}^L &= \frac{e(3 - 4s_W^2)}{6s_W c_W} , \quad g_{Zt}^R = \frac{-2es_W}{3c_W} \end{aligned} \quad (\text{A.3})$$

denote the usual SM couplings.

Neglecting  $m_e$ , there exist only four independent HC amplitudes  $F_{-++-}$ ,  $F_{+--+}$ ,  $F_{-+-+}$ ,  $F_{-++-}$  to be considered, whose Born contributions at high energies are

$$\begin{aligned} F_{-++-}^{\text{Born}} &\simeq e^2 \left( \frac{2u}{s} \right) \left( \frac{-3 + 2s_W^2}{12s_W^2 c_W^2} \right) , \quad F_{+--+}^{\text{Born}} \simeq e^2 \left( \frac{2u}{s} \right) \left( \frac{-2}{3c_W^2} \right) , \\ F_{-+-+}^{\text{Born}} &\simeq e^2 \left( \frac{2t}{s} \right) \left( \frac{-1}{3c_W^2} \right) , \quad F_{-++-}^{\text{Born}} \simeq e^2 \left( \frac{2t}{s} \right) \left( \frac{-1}{6c_W^2} \right) . \end{aligned} \quad (\text{A.4})$$

## A.1 The supersimple augmented Sudakov amplitudes.

The high energy supersimple expressions for the Sudakov part of the HC amplitudes, at the 1loop EW order, are

$$\begin{aligned}
F_{-++-}^{\text{Sud}} \simeq & \frac{2u\alpha^2}{s} \left\{ \frac{(9 - 12s_W^2 + 4s_W^4)}{144s_W^4c_W^4} \left[ \frac{(u-t)}{u} (\ln^2 r_{ts} + \pi^2) - 2\ln^2 t_Z + 2\ln^2 u_Z \right] \right. \\
& - \frac{(45 - 84s_W^2 + 40s_W^4)}{72s_W^4c_W^4} (\ln^2 r_{us} + \pi^2) + \frac{1}{2s_W^4} \left[ \ln^2 u_W + 2L_{eW\nu} + 2L_{tWb} \right. \\
& - \frac{1}{2} \overline{\ln(s_{W\nu})} - 2\overline{\ln(s_{WW})} - \frac{1}{2} \overline{\ln(s_{Wb})} \left. \right] \\
& - \frac{(3 - 4s_W^2)}{24s_W^4c_W^2} \left[ 2\ln^2 s_W + 4L_{eW\nu} - 3\overline{\ln(s_{W\nu})} + 4L_{tZt} - 3\overline{\ln(s_{Zt})} \right] \\
& - \frac{(-3 + 2s_W^2)}{48s_W^4c_W^4} \left[ \ln^2 s_Z + 4L_{eZe} - 3\overline{\ln(s_{Ze})} \right] \\
& - \frac{(-27 + 42s_W^2 - 16s_W^4)}{432s_W^4c_W^4} \left[ \ln^2 s_Z + 4L_{tZt} - 3\overline{\ln(s_{Zt})} \right] \\
& + \frac{(3 - 2s_W^2)}{48s_W^4c_W^4} \sum_i \left[ |Z_{1i}^N s_W + Z_{2i}^N c_W|^2 \overline{\ln(s_{\tilde{\chi}_i^0 \tilde{e}_L})} + \frac{|Z_{1i}^N s_W + 3Z_{2i}^N c_W|^2}{9} \overline{\ln(s_{\tilde{\chi}_i^0 \tilde{t}_L})} \right] \\
& + \frac{(3 - 5s_W^2 + 2s_W^4)}{24s_W^4c_W^4} \sum_i |Z_{1i}^+|^2 \overline{\ln(s_{\tilde{\chi}_i^+ \tilde{\nu}_L})} + \frac{(3 - 2s_W^2)}{24s_W^4c_W^2} \sum_i |Z_{1i}^-|^2 \overline{\ln(s_{\tilde{\chi}_i^+ \tilde{b}_L})} \\
& + \frac{(3 - 2s_W^2)}{24s_W^2c_W^2} \left[ \frac{m_t^2}{2s_W^2m_W^2\sin^2\beta} \sum_i |Z_{4i}^N|^2 \overline{\ln(s_{\tilde{\chi}_i^0 \tilde{t}_R})} + \frac{m_b^2}{2s_W^2m_W^2\cos^2\beta} \sum_i |Z_{2i}^+|^2 \overline{\ln(s_{\tilde{\chi}_i^+ \tilde{b}_R})} \right] \\
& + \frac{3 - 2s_W^2}{48s_W^2c_W^2} \left[ \frac{m_t^2}{2s_W^2m_W^2} \left( \frac{\sin^2\alpha}{\sin^2\beta} \overline{\ln(s_{tH^0})} + \frac{\cos^2\alpha}{\sin^2\beta} \overline{\ln(s_{th^0})} + \frac{\cos^2\beta}{\sin^2\beta} \overline{\ln(s_{tA^0})} + \overline{\ln(s_{tG^0})} \right) \right. \\
& \left. + \frac{m_b^2}{s_W^2m_W^2} \left( \tan^2\beta \overline{\ln(s_{bH^+})} + \overline{\ln(s_{bG^+})} \right) \right] \left. \right\} , \tag{A.5}
\end{aligned}$$

$$\begin{aligned}
F_{+--+}^{\text{Sud}} \simeq & \frac{2u\alpha^2}{s} \left\{ \frac{4}{9c_W^4} \left[ \frac{(u-t)}{u} (\ln^2 r_{ts} + \pi^2) - 2(\ln^2 r_{us} + \pi^2 + \ln^2 t_Z - \ln^2 u_Z) \right] \right. \\
& + \frac{2}{3c_W^4} \left[ \ln^2 s_Z + 4L_{eZe} - 3\overline{\ln(s_{Ze})} + \frac{4}{9} [\ln^2 s_Z + 4L_{tZt} - 3\overline{\ln(s_{Zt})}] \right] \\
& + \frac{2}{3c_W^4} \sum_i \left[ |Z_{1i}^N|^2 \overline{\ln(s_{\tilde{\chi}_i^0 \tilde{e}_R})} + \frac{4}{9} |Z_{1i}^N|^2 \overline{\ln(s_{\tilde{\chi}_i^0 \tilde{t}_R})} \right] \\
& + \frac{m_t^2}{6s_W^2c_W^2m_W^2\sin^2\beta} \sum_i \left[ |Z_{4i}^N|^2 \overline{\ln(s_{\tilde{\chi}_i^0 \tilde{t}_L})} + |Z_{2i}^+|^2 \overline{\ln(s_{\tilde{\chi}_i^+ \tilde{b}_L})} \right] \\
& + \frac{m_t^2}{12s_W^2c_W^2m_W^2} \left[ \frac{\sin^2\alpha}{\sin^2\beta} \overline{\ln(s_{tH^0})} + \frac{\cos^2\alpha}{\sin^2\beta} \overline{\ln(s_{th^0})} + \frac{\cos^2\beta}{\sin^2\beta} \overline{\ln(s_{tA^0})} + \overline{\ln(s_{tG^0})} \right]
\end{aligned}$$

$$+2 \cot^2 \beta \overline{\ln(s_{bH^+})} + 2 \overline{\ln(s_{bG^+})} \Big] \Big\} , \quad (\text{A.6})$$

$$\begin{aligned}
F_{-++-}^{\text{Sud}} \simeq & \frac{-2t\alpha^2}{s} \Big\{ \frac{1}{9c_W^4} \Big[ -2(\ln^2 r_{ts} + \pi^2) + \frac{(t-u)}{t}(\ln^2 r_{us} + \pi^2) + 2\ln^2 t_Z - 2\ln^2 u_Z \Big] \\
& - \frac{1}{12s_W^2 c_W^4} \Big[ \ln^2 s_Z + 4L_{eZe} - 3\overline{\ln(s_{Ze})} + \frac{16s_W^2}{9} \Big( \ln^2 s_Z + 4L_{tZt} - 3\overline{\ln(s_{Zt})} \Big) \Big] \\
& - \frac{1}{6s_W^2 c_W^2} \Big[ \ln^2 s_W + 4L_{eW\nu} - 3\overline{\ln(s_{W\nu})} \Big] \\
& - \frac{1}{12s_W^2 c_W^4} \sum_i \Big[ \Big| Z_{1i}^N s_W + Z_{2i}^N c_W \Big|^2 \overline{\ln(s_{\tilde{\chi}_i^0 \tilde{e}_L})} + \frac{16s_W^2}{9} |Z_{1i}^N|^2 \overline{\ln(s_{\tilde{\chi}_i^0 \tilde{t}_R})} \Big] \\
& - \frac{1}{6s_W^2 c_W^2} \sum_i |Z_{1i}^+|^2 \overline{\ln(s_{\tilde{\chi}_i^+ \tilde{\nu}_L})} - \frac{m_t^2}{12s_W^2 c_W^2 m_W^2 \sin^2 \beta} \sum_i \Big[ |Z_{4i}^N|^2 \overline{\ln(s_{\tilde{\chi}_i^0 \tilde{t}_L})} + |Z_{2i}^+|^2 \overline{\ln(s_{\tilde{\chi}_i^+ \tilde{b}_L})} \Big] \\
& - \frac{m_t^2}{24s_W^2 c_W^2 m_W^2} \Big[ \frac{\sin^2 \alpha}{\sin^2 \beta} \overline{\ln(s_{tH^0})} + \frac{\cos^2 \alpha}{\sin^2 \beta} \overline{\ln(s_{th^0})} + \frac{\cos^2 \beta}{\sin^2 \beta} \overline{\ln(s_{tA^0})} + \overline{\ln(s_{tG^0})} \\
& + 2 \cot^2 \beta \overline{\ln(s_{bH^+})} + 2 \overline{\ln(s_{bG^+})} \Big] \Big\} , \quad (\text{A.7})
\end{aligned}$$

$$\begin{aligned}
F_{+--+}^{\text{Sud}} \simeq & \frac{-2t\alpha^2}{s} \Big\{ \frac{1}{36c_W^4} \Big[ -2(\ln^2 r_{ts} + \pi^2) + \frac{(t-u)}{t}(\ln^2 r_{us} + \pi^2) + 2\ln^2 t_Z - 2\ln^2 u_Z \Big] \\
& - \frac{1}{6c_W^4} \Big[ \ln^2 s_Z + 4L_{eZe} - 3\overline{\ln(s_{Ze})} \Big] - \frac{(9-8s_W^2)}{216s_W^2 c_W^4} \Big[ \ln^2 s_Z + 4L_{tZt} - 3\overline{\ln(s_{Zt})} \Big] \\
& - \frac{1}{12s_W^2 c_W^2} \Big[ \ln^2 s_W + 4L_{tWb} - 3\overline{\ln(s_{Wb})} \Big] \\
& - \frac{1}{6c_W^4} \sum_i \Big[ |Z_{1i}^N|^2 \overline{\ln(s_{\tilde{\chi}_i^0 \tilde{e}_R})} + \frac{1}{36s_W^2} |Z_{1i}^N s_W + 3Z_{2i}^N c_W|^2 \overline{\ln(s_{\tilde{\chi}_i^0 \tilde{t}_L})} \Big] \\
& - \frac{1}{12s_W^2 c_W^2} \sum_i \Big[ |Z_{1i}^-|^2 \overline{\ln(s_{\tilde{\chi}_i^- \tilde{b}_L})} + \frac{m_t^2 |Z_{4i}^N|^2}{2m_W^2 \sin^2 \beta} \overline{\ln(s_{\tilde{\chi}_i^0 \tilde{t}_R})} + \frac{m_b^2 |Z_{2i}^+|^2}{2m_W^2 \cos^2 \beta} \overline{\ln(s_{\tilde{\chi}_i^+ \tilde{b}_R})} \Big] \\
& - \frac{m_t^2}{48s_W^2 c_W^2 m_W^2} \Big[ \frac{\sin^2 \alpha}{\sin^2 \beta} \overline{\ln(s_{tH^0})} + \frac{\cos^2 \alpha}{\sin^2 \beta} \overline{\ln(s_{th^0})} + \frac{\cos^2 \beta}{\sin^2 \beta} \overline{\ln(s_{tA^0})} + \overline{\ln(s_{tG^0})} \Big] \\
& - \frac{m_b^2}{24s_W^2 c_W^2 m_W^2} \Big[ \tan^2 \beta \overline{\ln(s_{bH^+})} + \overline{\ln(s_{bG^+})} \Big] \Big\} \quad (\text{A.8})
\end{aligned}$$

where the chargino and neutralino mixing matrices ( $Z^N, Z^+, Z^-$ ) are as in [26],

Note that all high energy supersimple expressions (A.5-A.8) are solely expressed as linear combinations of the forms (6, 7, 8), with the coefficients of (6, 7) being constants satisfying the general constraints [5, 6, 7, 8]. The coefficients of the forms (8) though, may also involve ratios of Mandelstam variables [1]. No additional constants appear in (A.5-A.8); i.e. there are no additional residual terms in them.



We also remark that the pinch contribution which only affects  $F_{-++}$ , has been put in  $F_{-++}^{\text{s.e.}}$ , as discussed in Sect 2.

Notice also that for the  $e^-e^+ \rightarrow t\bar{t}$ , the structure of (6,9,10) implies that

$$\ln^2 t_Z - \ln^2 u_Z = \overline{\ln^2 t_Z} - \overline{\ln^2 u_Z} , \quad (\text{A.9})$$

so that all  $\ln^2(x_V)$  terms in (A.5-A.8) with  $(x = s, t, u)$ , are consistent with the form (6).

Moreover, since we are using a Feynman-t'Hooft gauge, the masses of the charged and neutral Goldstone bosons (whenever they appear in the equations above) are taken as  $m_W$  and  $m_Z$  respectively.

Finally, (A.5-A.8) clearly indicate that the Yukawa interactions do respect the supersimplicity structure.

## A.2 The supersimple augmented RG amplitudes.

At high energies the  $\gamma\gamma, \gamma Z, ZZ$  renormalized self-energy contribution to the four HC helicity amplitudes, together with the pinch contribution, are

$$F_{-++}^{\text{s.e.}} \simeq -\frac{2u}{s^2} \sum_{V,V'} \hat{\Sigma}_{VV'}(s) g_{Ve}^L g_{V't}^L + \frac{\alpha^2}{s_W^4} \overline{\ln s_W W} , \quad (\text{A.10})$$

$$F_{+-+}^{\text{s.e.}} \simeq -\frac{2u}{s^2} \sum_{V,V'} \hat{\Sigma}_{VV'}(s) g_{Ve}^R g_{V't}^R , \quad (\text{A.11})$$

$$F_{-+-}^{\text{s.e.}} \simeq -\frac{2t}{s^2} \sum_{V,V'} \hat{\Sigma}_{VV'}(s) g_{Ve}^L g_{V't}^R , \quad (\text{A.12})$$

$$F_{+--}^{\text{s.e.}} \simeq -\frac{2t}{s^2} \sum_{V,V'} \hat{\Sigma}_{VV'}(s) g_{Ve}^R g_{V't}^L , \quad (\text{A.13})$$

where  $V$  and  $V'$  run over  $\gamma$  and  $Z$ , and the coupling constants are given in (A.3). The last term in (A.10) is the aforementioned pinch contribution (14).

We next discuss the renormalized gauge self-energy functions  $\hat{\Sigma}_{VV'}(s)$ . In the on-shell scheme we have (for details and notations see [4])

$$\begin{aligned} \hat{\Sigma}_{\gamma\gamma}(s) &= \Sigma_{\gamma\gamma}(s) + s\delta Z_2^\gamma , \\ \hat{\Sigma}_{ZZ}(s) &= \Sigma_{ZZ}(s) - \delta m_Z^2 + (s - m_Z^2)\delta Z_2^Z , \\ \hat{\Sigma}_{\gamma Z}(s) &= \Sigma_{\gamma Z}(s) + s\delta Z_2^{\gamma Z} + m_Z^2(\delta Z_1^{\gamma Z} - \delta Z_2^{\gamma Z}) , \end{aligned} \quad (\text{A.14})$$

where

$$\begin{aligned} \delta Z_2^\gamma &= -\Sigma'_{\gamma\gamma}(0) , \quad \delta Z_1^\gamma = -\Sigma'_{\gamma\gamma}(0) + \frac{s_W}{c_W} \frac{\Sigma_{\gamma Z}(0)}{m_Z^2} , \\ \delta Z_2^Z &= -\Sigma'_{\gamma\gamma}(0) + 2 \frac{c_W^2 - s_W^2}{s_W c_W} \frac{\Sigma_{\gamma Z}(0)}{m_Z^2} + \frac{c_W^2 - s_W^2}{s_W^2} \left( \frac{\delta m_Z^2}{m_Z^2} - \frac{\delta m_W^2}{m_W^2} \right) , \end{aligned}$$

$$\begin{aligned}
\delta Z_1^Z &= -\Sigma'_{\gamma\gamma}(0) + \frac{3c_W^2 - 2s_W^2}{s_W c_W} \frac{\Sigma_{\gamma Z}(0)}{m_Z^2} + \frac{c_W^2 - s_W^2}{s_W^2} \left( \frac{\delta m_Z^2}{m_Z^2} - \frac{\delta m_W^2}{m_W^2} \right) , \\
\delta Z_i^{\gamma Z} &= \frac{c_W s_W}{c_W^2 - s_W^2} (\delta Z_i^Z - \delta Z_i^\gamma) , \\
\delta M_W^2 &= \text{Re} \Sigma_{WW}(M_W^2) , \quad \delta M_Z^2 = \text{Re} \Sigma_{ZZ}(M_Z^2) .
\end{aligned} \tag{A.15}$$

At high energies, (A.14) become

$$\begin{aligned}
\hat{\Sigma}_{\gamma\gamma}(s) &\simeq \Sigma_{\gamma\gamma}(s) + s \delta Z_2^\gamma , \\
\hat{\Sigma}_{ZZ}(s) &\simeq \Sigma_{ZZ}(s) + s \delta Z_2^Z , \\
\hat{\Sigma}_{\gamma Z}(s) &\simeq \Sigma_{\gamma Z}(s) + s \delta Z_2^{\gamma Z} .
\end{aligned} \tag{A.16}$$

Using then the definitions (7,13), we obtain the supersimple high energy expressions

$$\begin{aligned}
\hat{\Sigma}_{\gamma\gamma}(s) &\simeq \frac{s\alpha}{\pi} \left\{ \frac{3}{4} \overline{\ln(s_{W+W^-})} - \frac{1}{12} \overline{\ln(s_{H+H^-})} \right. \\
&\quad \left. - \sum_f N_c^f Q_f^2 \frac{1}{3} \left[ \overline{\ln(s_{f\bar{f}})} + \frac{1}{4} \sum_i \overline{\ln(s_{\tilde{f}_i \tilde{f}_i})} \right] - \frac{1}{3} \sum_{\tilde{\chi}_j} \overline{\ln(s_{\tilde{\chi}_j^+ \tilde{\chi}_j^-})} \right\} ,
\end{aligned} \tag{A.17}$$

$$\begin{aligned}
\hat{\Sigma}_{\gamma Z}(s) &\simeq -\frac{s\alpha}{\pi} \left\{ \frac{\cos(2\theta_W)}{24 s_W c_W} \left[ \overline{\ln(s_{H+H^-})} + \overline{\ln(s_{W+W^-})} \right] - \frac{5c_W}{6s_W} \overline{\ln(s_{W+W^-})} \right. \\
&\quad + \sum_f N_c^f Q_f \frac{v_f}{3} \overline{\ln(s_{f\bar{f}})} + \frac{1}{12 s_W c_W} \sum_f N_c^f Q_f \left\{ (I_3^f c_{\theta_f}^2 - Q_f s_W^2) \overline{\ln(s_{\tilde{f}_1 \tilde{f}_1})} \right. \\
&\quad \left. + (I_3^f s_{\theta_f}^2 - Q_f s_W^2) \overline{\ln(s_{\tilde{f}_2 \tilde{f}_2})} \right\} + \frac{1}{12 s_W c_W} \sum_{j=1}^2 (O_{jj}^{ZL} + O_{jj}^{ZR}) \overline{\ln(s_{\tilde{\chi}_j^+ \tilde{\chi}_j^-})} \left. \right\} \\
&\quad + s \frac{c_W}{s_W} \overline{\Delta\rho} ,
\end{aligned} \tag{A.18}$$

$$\begin{aligned}
\hat{\Sigma}_{ZZ}(s) &\simeq \frac{s\alpha}{\pi} \left\{ \frac{1}{4 s_W^2 c_W^2} \left[ -\frac{\sin^2(\beta - \alpha)}{12} \left( \overline{\ln(s_{hZ})} + \overline{\ln(s_{H^0 A^0})} \right) \right. \right. \\
&\quad \left. \left. - \frac{\cos^2(\beta - \alpha)}{12} \left( \overline{\ln(s_{H^0 Z})} + \overline{\ln(s_{h A^0})} \right) \right] \right. \\
&\quad - \frac{\cos^2(2\theta_W)}{12} \overline{\ln(s_{H+H^-})} + \left( \frac{10}{3} c_W^4 - \frac{\cos^2(2\theta_W)}{12} \right) \overline{\ln(s_{W+W^-})} \\
&\quad - \sum_f N_c^f \left\{ \frac{(v_f^2 + a_f^2)}{3} \overline{\ln(s_{f\bar{f}})} - \frac{1}{48 s_W^2 c_W^2} \sum_f N_c^f \left\{ 4[I_3^f c_{\theta_f}^2 - Q_f s_W^2]^2 \overline{\ln(s_{\tilde{f}_1 \tilde{f}_1})} \right. \right. \\
&\quad \left. \left. + s_{\theta_f}^2 c_{\theta_f}^2 (\overline{\ln(s_{\tilde{f}_1 \tilde{f}_2})} + \overline{\ln(s_{\tilde{f}_2 \tilde{f}_1})}) + 4[I_3^f s_{\theta_f}^2 - Q_f s_W^2]^2 \overline{\ln(s_{\tilde{f}_2 \tilde{f}_2})} \right\} \right.
\end{aligned}$$

$$\begin{aligned}
& + \frac{1}{24s_W^2 c_W^2} \left[ \sum_{i,j=1}^4 O_{ji}^{0ZL} O_{ij}^{0ZL} \overline{\ln(s_{\tilde{\chi}_i^0 \tilde{\chi}_j^0})} \right. \\
& \left. - \sum_{i,j=1}^2 \left( O_{ij}^{ZL} O_{ji}^{ZL} + O_{ij}^{ZR} O_{ji}^{ZR} \right) \overline{\ln(s_{\tilde{\chi}_i^+ \tilde{\chi}_j^-})} \right] \Big\} + s \frac{c_W^2 - s_W^2}{s_W^2} \overline{\Delta\rho} \quad , \quad (A.19)
\end{aligned}$$

where  $\tilde{\theta}_f$  denotes the  $(\tilde{f}_L, \tilde{f}_R)$ -sfermion mixing angle, and

$$\begin{aligned}
O_{ij}^{0ZL} &= O_{ji}^{0ZL*} = -O_{ji}^{0ZR} = -O_{ij}^{0ZR*} = Z_{4i}^{N*} Z_{4j}^N - Z_{3i}^{N*} Z_{3j}^N \quad , \\
O_{ij}^{ZL} &= Z_{1i}^{+*} Z_{1j}^+ + \delta_{ij} (c_W^2 - s_W^2) \quad , \\
O_{ij}^{ZR} &= Z_{1i}^- Z_{1j}^{-*} + \delta_{ij} (c_W^2 - s_W^2) \quad , \quad (A.20)
\end{aligned}$$

with the  $(Z^N, Z^+, Z^-)$  matrices being as in Appendix A.1. Finally

$$v_f = \frac{I_3^f - 2Q_f s_W^2}{2s_W c_W} \quad , \quad a_f = \frac{I_3^f}{2s_W c_W} \quad , \quad (A.21)$$

with  $I_3^f$  being the third component of the isospin of the L-fermion or sfermion fields, and  $Q_f$  the corresponding electric charge. In all cases, CP conserving SUSY couplings are assumed.

It is worth remarking, that the high energy expressions (A.10-A.13) for the RG amplitudes, do respect the supersimplicity structure. In this respect we note that in addition to the forms (6, 7, 8), they also contain residual constant contributions given by  $\overline{\Delta\rho}$  in (A.18,A.19) and further discussed in Sect.3.2.

## B Appendix: Anomalous effective $Zt\bar{t}$ coupling and $Z'$ effects

Here we define the two new-physics models, used for illustration in Fig.7 and Table 1.

The first such model just contains the additional effective  $Zt\bar{t}$  coupling

$$- ie \frac{d^Z}{m_t} \epsilon^Z \cdot (p - p') \quad , \quad (B.1)$$

where  $p, p'$  denote the  $t, \bar{t}$  momenta respectively; while  $d^Z$  is an effective coupling, (which a priori could also be s-dependent). Such an interaction leads to the additional helicity amplitudes

$$F_{\lambda, \lambda', \mu, \mu'}^{d^Z} = - \frac{\lambda e^2 d^Z s^{3/2}}{2m_t s_W^2 c_W^2 (s - m_Z^2)} \left( 1 - \frac{m_t^2}{s} \right)^2 \sin \theta \delta_{\mu, \mu'} \left[ g_{Ze}^L \delta_{\lambda, -\frac{1}{2}} + g_{Ze}^R \delta_{\lambda, +\frac{1}{2}} \right] \quad , \quad (B.2)$$

where (1, 2, A.3) are used. As seen from (B.2),  $d^Z$ -contributions only exist for the helicity violating amplitudes  $F_{-+--}$ ,  $F_{-+++}$ ,  $F_{+---}$ ,  $F_{+--+}$ .

The second new-physics model used in Table 1, just contains a new vector boson  $Z'$ , with common, purely vector or axial couplings, to all fermions. It is described by the vertex

$$-ie\gamma^\nu [g_{Z'f}^v Z'_\nu(V) - g_{Z'f}^a \gamma_5 Z'_\nu(A)] \quad . \quad (\text{B.3})$$

In Table 1, common couplings, for both  $f = e$  and  $f = t$  cases have been used, for purely vector (axial) couplings chosen as  $g_{Z'f}^v = 1$  ( $g_{Z'f}^a = 1$ ). The  $Z'$ -mass is taken as 3TeV.

## References

- [1] G.J. Gounaris and F.M. Renard, Acta Phys. Polon. **42**, 2107 (2011) , arXiv:1106.2707[hep-ph].
- [2] G.J. Gounaris and F.M. Renard, Phys. Rev. Lett. **94**, 131601 (2005), hep-ph/0501046.
- [3] G.J. Gounaris and F.M. Renard, Phys. Rev. **D73**, 097301 (2006), hep-ph/0604041, (an Addendum).
- [4] W. Hollik, Fortsch. Phys. **38**, 165 (1990).
- [5] M. Beccaria, F.M. Renard and C. Verzegnassi, hep-ph/0203254, "Logarithmic Fingerprints of Virtual Supersymmetry", Linear Collider note LC-TH-2002-005, GDR Supersymmetrie note GDR-S-081.
- [6] M. Beccaria, M. Melles, F. M. Renard, S. Trimarchi, C. Verzegnassi, Int. J. Mod. Phys. **A18**, 5069 (2003), hep-ph/0304110.
- [7] M. Beccaria, F.M. Renard and C. Verzegnassi, hep-ph/0904.2646; Int. J. Mod. Phys. **A24**, 6123 (2009).
- [8] M. Beccaria, E. Mirabella, Phys. Rev. **D71**, 115016 (2005), [hep-ph/0505172].
- [9] M. Jacob and G.C. Wick, Annals of Phys. **7**, 404 (1959), Annals of Phys. **281**, 774 (2000)
- [10] D. Chang, W-Y. Keung, and I. Phillips, Nucl. Phys. **B408**, 286 (1993).
- [11] G.J. Gounaris, J. Layssac, F.M. Renard, Phys. Rev. **D55**, 5786 (1997), hep-ph/9612335.
- [12] G. Degrassi and A. Sirlin, Nucl. Phys. **B383**, 73 (1992), Phys. Rev. **D46**, 3104 (1992).
- [13] D. Binosi and J. Papavassiliou Phys. Rep. **479**, 1 (2009), arXiv:0909.2536 [hep-ph].
- [14] M. Beccaria, F.M. Renard and C. Verzegnassi, Phys. Rev. **D63**, 053013 (2001).
- [15] M. Beccaria, G.J. Gounaris, J. Layssac and F.M. Renard, Int. J. Mod. Phys. **A23**, 1839 (2008).
- [16] G. Passarino and M. Veltman Nucl. Phys. **B160**, 151 (1979).
- [17] O. Buchmueller et al, arXiv:1112.3564[hep-ph].
- [18] "SuSpect", A. Djouadi, J.-L. Kneur and G. Moultaka, hep-ph/0211331.

- [19] S. Heinemeyer, O. Stal, G. Weiglein Phys. Lett. **B710**, 201 (2012), arXiv:1112.3026 [hep-ph].
- [20] L. Maiani, A.D. Polosa, V. Riquer, arXiv:1202.5998 [hep-ph].
- [21] M. Davier, A. Hoecker, B. Malaescu, et al., Eur. Phys. J. **C71**, 1515 (2011), arXiv:1010.4180.
- [22] K. Hagiwara, R. Liao, A. D. Martin, et al., J. Phys. **G38**, 085003 (2011), arXiv:1105.3149.
- [23] H.Baer, V. Barger, A. Mustafayev, arXiv:1112.3017[hep-ph]; S. Akula, B. Altunkaynak, D. Feldman, P. Nath and G. Peim, arXiv:1112.3645[hep-ph]; A. Arbey et al Phys. Lett. **B708**, 162 (2012), arXiv:1112.3028 [hep-ph].
- [24] T. Aaltonen et al.(CDF), Phys.Rev.D83(2011)112003; arxiv: 1101.0034.
- [25] V.M. Abazov et al.(D0), Phys.Rev.D84(2011)112005; arxiv: 1107.4995.
- [26] J. Rosiek, Phys. Rev. **D41**, 3464 (1990).

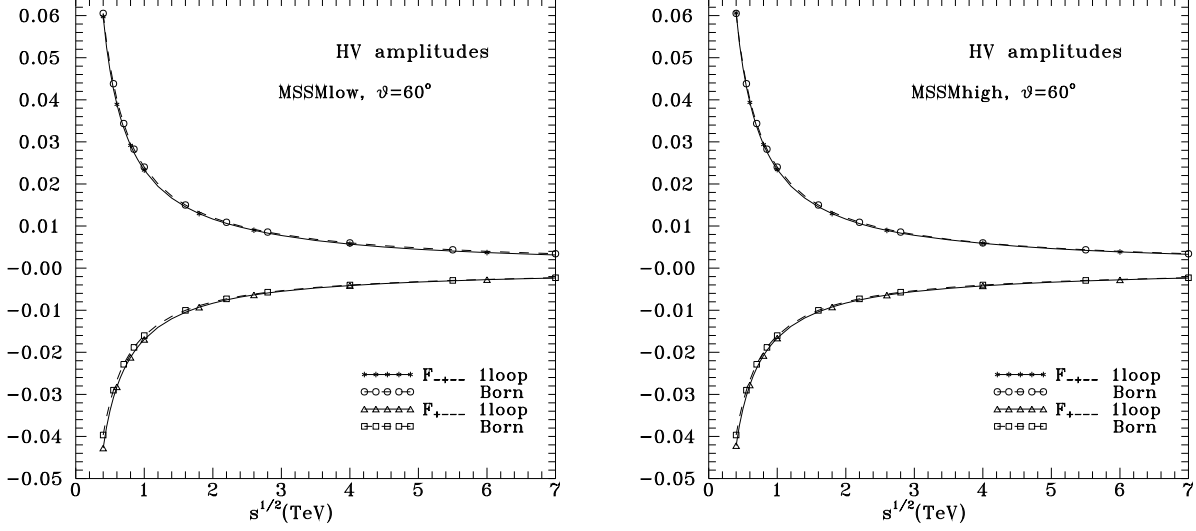


Figure 2: Energy dependence at  $\theta = 60^\circ$ , of the HV amplitudes  $F_{-+--}$  and  $F_{+---}$ , at the 1loop EW order and their Born approximation. Left panel corresponds to MSSMlow, defined in (17), and right panel corresponds to MSSMhigh, defined in (16).

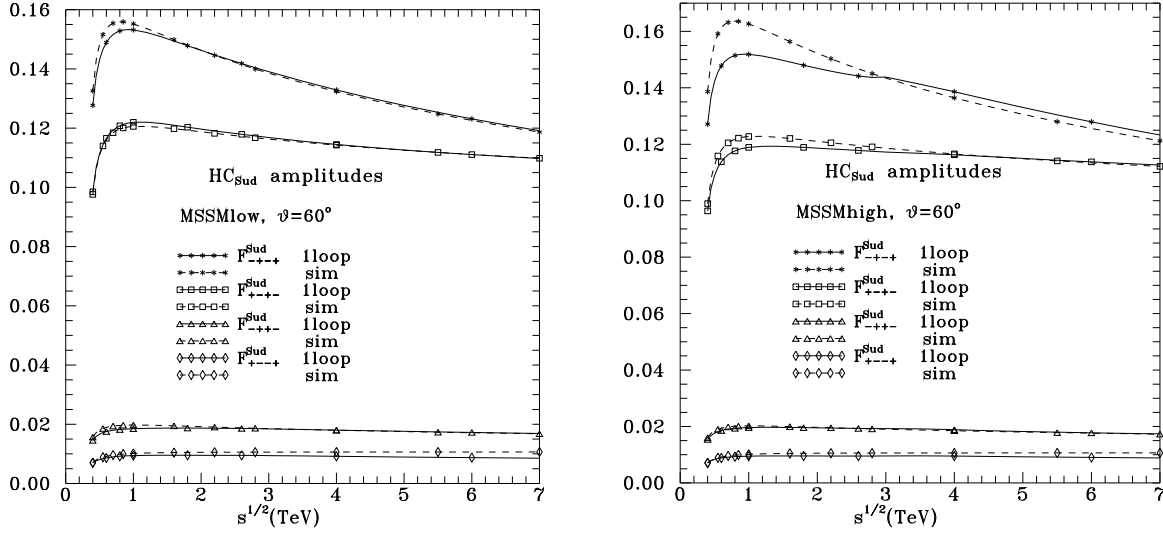


Figure 3: Energy dependence at  $\theta = 60^\circ$ , of the augmented Sudakov part of the HC amplitudes  $F_{-+--}^{\text{Sud}}$ ,  $F_{+---}^{\text{Sud}}$ ,  $F_{-++-}^{\text{Sud}}$ ,  $F_{+-+-}^{\text{Sud}}$ . Full lines describe the exact 1loop EW order results; while broken lines, indicated by "sim", denote the supersimple high energy approximation given in Appendix A.1. Panels and models as in Fig.2.

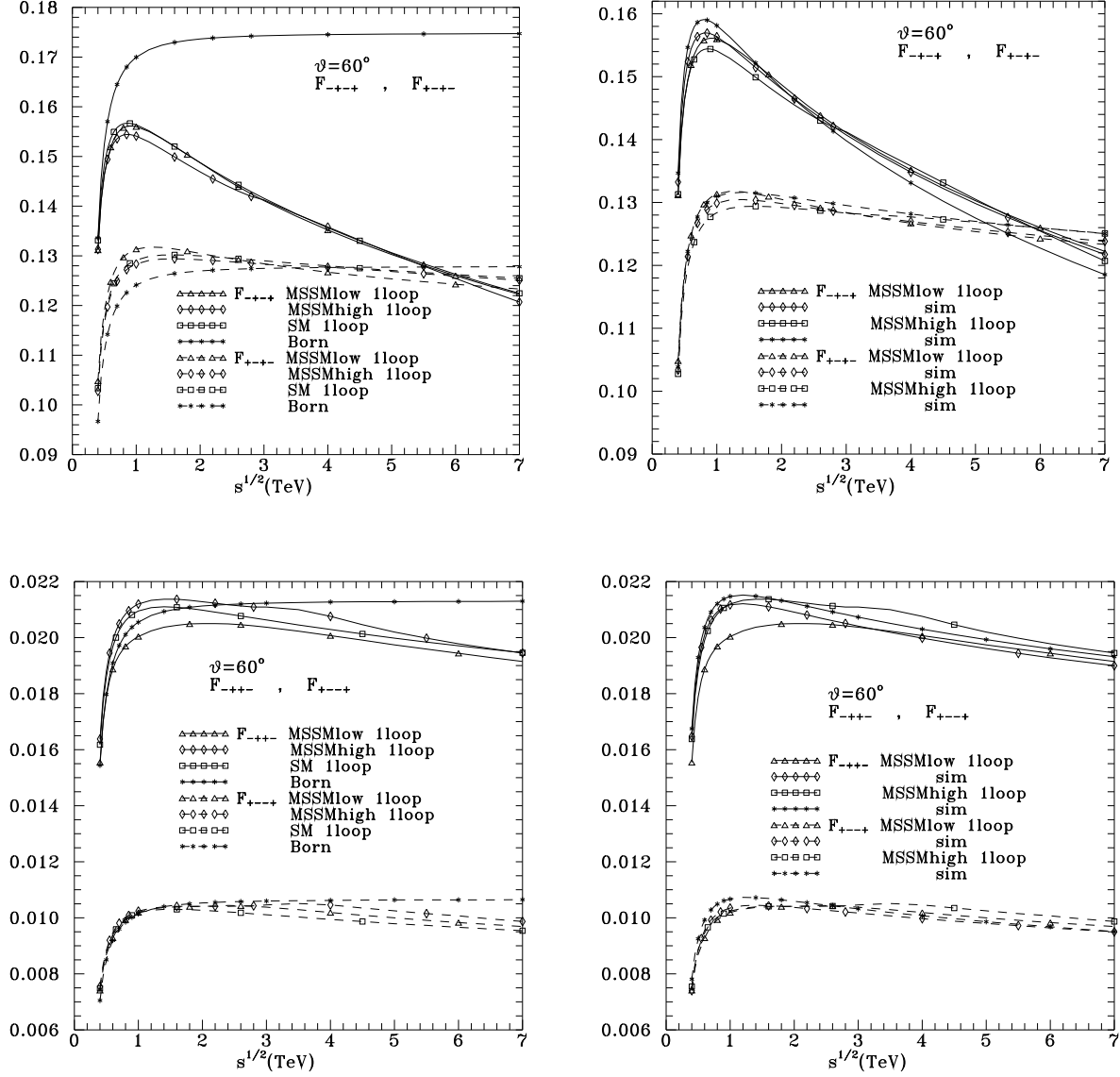


Figure 4: Energy dependence at  $\theta = 60^\circ$ , of the complete HC amplitudes  $F_{-++-}$ ,  $F_{+--+}$  (upper panels), and  $F_{-+-+}$ ,  $F_{+--+}$  (lower panels). Models as in caption of Fig.2. Left panels show the exact 1loop effects on Born, in SM and MSSM. Right panels show the accuracy of the supersimple expressions of Appendix A, indicated by "sim".



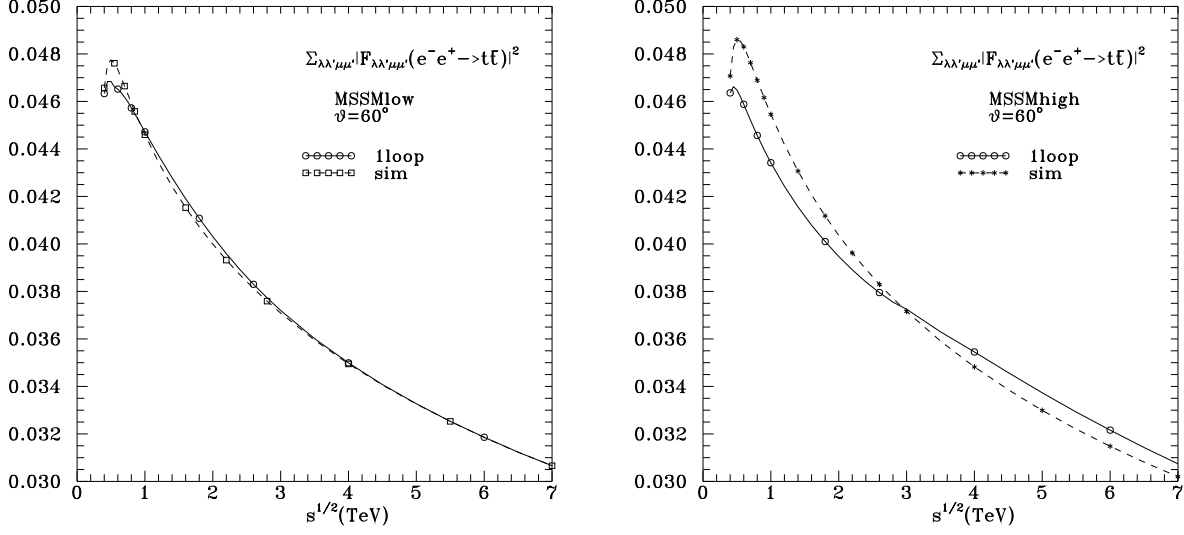


Figure 5: Energy dependence for the "dimensionless cross section" in (28). Full lines describe the 1loop EW order results, while broken lines describe the "sim" results determined as stated just after (28). Models and panels as in Fig.2.

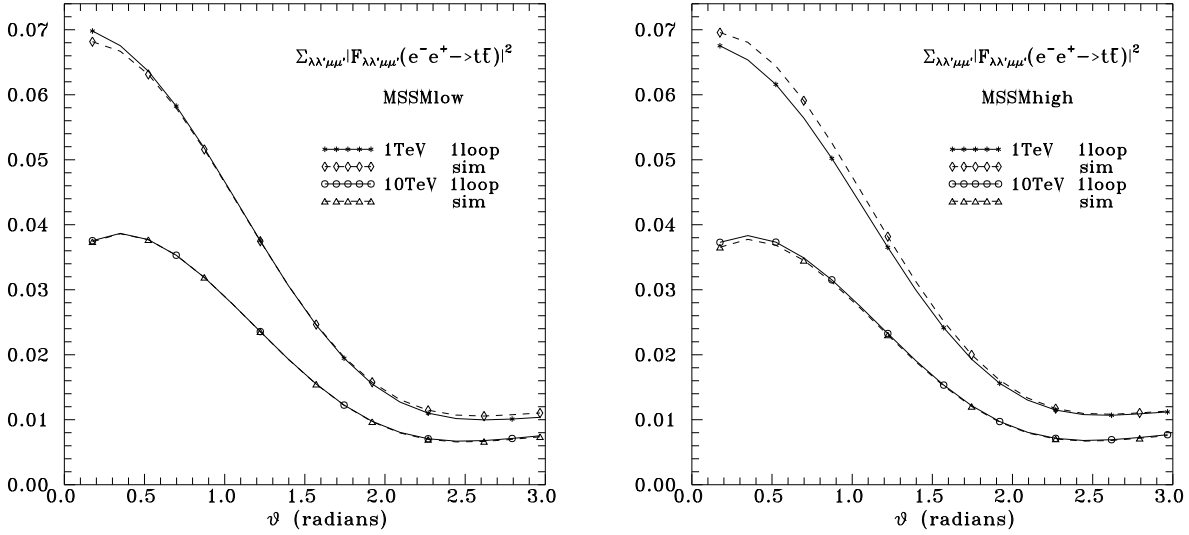


Figure 6: Angular dependence for the "dimensionless cross section" in (28), at c.m. energies of 1 and 10 TeV. Full lines describe the 1loop EW order results, while broken lines describe the "sim" results determined as stated just after (28). Models and panels as in Fig.2.

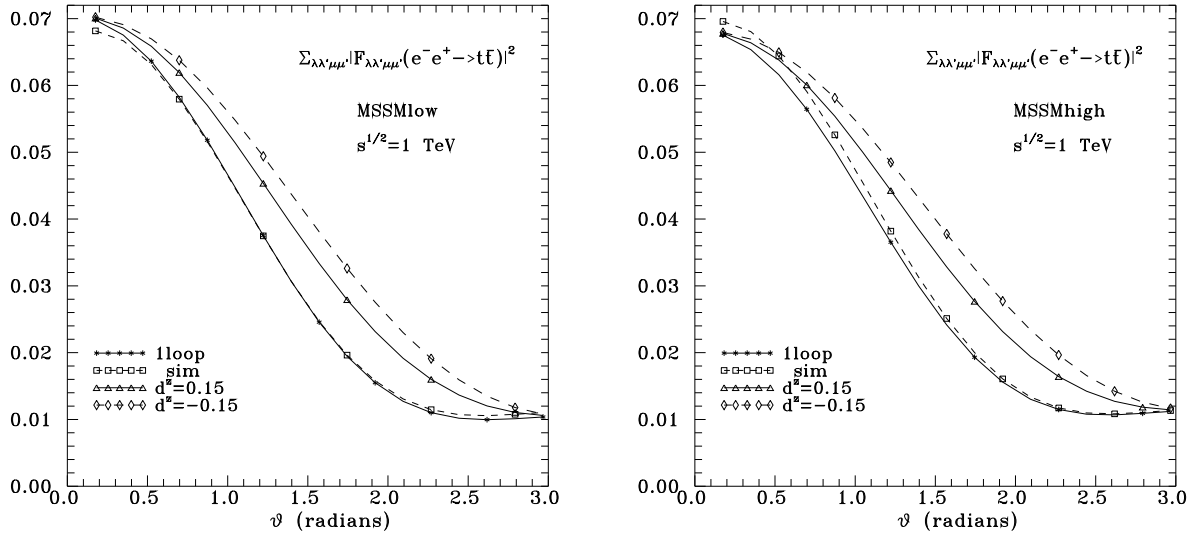


Figure 7: Angular dependence for the "dimensionless cross section" in (28) and the two MSSM benchmarks (17,16), at 1 TeV. Results including in addition the anomalous  $Zt\bar{t}$  couplings in (B.1), are also shown. The "sim" predictions are described just after (28). Left panel corresponds to MSSMlow, and right panel to MSSMhigh.